Trees (2015) 29:961–972
DOI 10.1007/s00468-014-1144-5

ORIGINAL PAPER

Xylem hydraulic properties in subtropical coniferous trees influence radial patterns of sap flow: implications for whole tree transpiration estimates using sap flow sensors

Adrien Guyot · Kasper T. Ostergaard · Junliang Fan · Nadia S. Santini · David A. Lockington

Received: 5 June 2014 / Revised: 26 November 2014 / Accepted: 12 December 2014 / Published online: 21 December 2014

Abstract

Key message **A high spatial resolution dataset of sap flux density in subtropical conifers is used to assess the minimum number and location of sap flow sensors required to monitor tree transpiration accurately.**

Abstract Tree transpiration is commonly estimated by methods based on in situ sap flux density (SFD) measurements, where the upscaling of SFD from point measurements to the individual tree has been identified as the main source of error. The literature indicates that the variation in SFD with radial position across a tree stem section can exhibit a wide range of patterns. Adequate capture of the SFD profile may require a large number of point measurements, which is likely to be prohibited. Thus, it is of value to develop protocols, which rationalize the number of point measurements, while retaining a satisfactory precision in the tree SFD estimates. This study investigates cross-sectional SFD variability within a tree and successively for six individual trees within a stand of *Pinus elliottii* var. *elliottii* × *caribaea* var. *hondurensis* (PEE × PCH). The stand is part of a plantation in subtropical coastal Australia. SFD is estimated using the Heat Field Deformation method simultaneously for four cardinal directions with measurements at six depths from the cambium. This yields a reference value of single tree SFD based on the twenty-four point measurements. Large variability of SFD is observed with measurement depth, cardinal direction and selected tree. We suggest that this is linked to the occurrence of successive narrow early and latewood rings with contrasting-specific hydraulic conductivities and wood water contents. Thus, an accurate placement of sensors within each ring is difficult to achieve in the field with the sensor footprint covering several rings of both early and latewood. Based on the reference dataset, we identified both an "ideal" setup and an "optimal" setup in terms of cost effectiveness and accuracy. Our study shows the need of using a systematic protocol to optimize the number of sensors to be used as a trade-off between precision and cost. It includes a preliminary assessment of the SFD variability at a high spatial resolution, and only then based on this, an appropriate placement of sensors for the long-term monitoring.

Keywords *Pinus elliottii* × *caribaea* · Plant water relations · Sap flux density · Sapwood · Tree water use · Upscaling

Communicated by A. Franco.

A. Guyot · J. Fan · N. S. Santini · D. A. Lockington
National Centre for Groundwater Research and Training, Bedford Park, SA 5042, Australia

A. Guyot (✉) · K. T. Ostergaard · J. Fan · D. A. Lockington
School of Civil Engineering, The University of Queensland, St. Lucia QLD 4072, Australia
e-mail: a.guyot@uq.edu.au

N. S. Santini
University of Technology, Sydney, PO Box 123, Sydney, NSW 2007, Australia

Introduction

Accurate tree water use estimates (Wullschleger et al. 1998) are of interest in water resources management (Brauman et al. 2007) or to assess the role of transpiration in the eco-hydrology of forested systems (Wilson et al. 2001). Zhang et al. (2011) recently modeled the impact of conifer plantations on catchment water balance in Australia and showed the need of improving the accuracy in transpiration estimates. Conifer plantations are increasingly common around the world as their rapid growth rates make them a sustainable source of construction material (Kennedy 1995) and potential carbon sinks (Cannell 1999). However, the increasing pressures on water resources lead water managers to better quantify their water consumption efficiency as compared to natural forests. Only very few studies (e.g. Dye et al. 1991; Bubb and Croton 2002; Alvarado-Barrientos et al. 2013) have investigated subtropical conifer water use, even though substantial variability in tree hydraulic architecture has been observed for these species (Dye et al. 1991; Domec and Gartner 2002; Downes and Drew 2008).

Tree water use is commonly measured using sap flow sensors at defined locations across the tree stem; however, this technique presents uncertainty issues at the different stages of measurement and upscaling procedures (Clearwater et al. 1999). Sap flux density (SFD) variability across a cross-section of tree could lead to significant error in estimates of tree transpiration if not recorded and taken into account. Hatton et al. (1990) and more recently Cermak et al. (2004) have identified the upscaling of sap flux density from point measurement to the whole tree as being responsible for the most error when trying to quantify forest transpiration. Nadezhdina et al. (2002) found systematic errors of −50 to +300 % for *Pinus Sylvestris* L., when a uniform sap flow across the tree stem was assumed. Ford et al. (2004a, b) showed that single point estimates for *Pinus* spp. resulted in errors as large as 154 % as compared to multiple point measurement of sap flow.

Table 1 presents the results of studies of conifer SFD variability across the sapwood obtained using sap flow sensors. Approximately one-third found monotonic decreases of SFD with distance from the cambium, one-third found asymmetrical profiles, while a few observed other patterns, i.e. Gaussian or bimodal. This variation in the findings shows that it is necessary to develop a strategy to rationalize the number of sensors required to estimate tree water use. That is given that the number of sensors to be used is usually a trade-off between obtaining a reliable estimate and the lowest possible cost. We would like to identify a corresponding field approach, which allows for the a priori unknown SFD variation.

Hatton et al. (1990) proposed a "weighted average method", where single point measurements are integrated to the whole tree with a weighted average of each sap flux density with depth, corresponding to a proportion of each surface the flow is most likely to be associated with. Other authors (e.g. Oishi et al. (2008), Ford et al. (2004a, b), Caylor and Dragoni (2009), Dragoni et al. (2009)) have proposed that functions (Polynomial, Gaussian, or others) are fit to point measurements taken across the sapwood. If suitable, the function could be fit with the appropriate minimum number of data points and integrated over the cross-section of the tree for total sap flux. However, the authors such as Saveyn et al. (2008) have found that the variability in the sap flux density across the sapwood area is such that no useful function could be identified.

Phillips et al. (1996) hypothesize that static xylem hydraulic properties, as well as dynamic physiological adaptation to water storage and movement could create the observed variations in sap flux densities. They tried to link the observed patterns of sap flux densities to the wood properties (in terms of specific gravity and water content) of the main classes of trees: non-porous, ring porous and diffuse porous. However, they only focused on the difference in wood properties between the outer and inner xylem. Other authors (e.g. Dye et al. 1991; Gebauer et al. 2008) have proposed measurement strategies based on each species' physiology and wood anatomy. Steppe et al. (2010) have shown that there is considerable variability of sap flux density across the stem section even within the same species for the same tree using lab-controlled gravimetric flow.

A few studies investigated the optimal number of sensors and their location. Koestner et al. (1998) have shown that the use of 12 probes placed randomly across the sapwood kept their coefficient of variation at 15 % while as few as 6 were required when placed at stratified depth and quadrant within their single *Eucalyptus* tree. Hatton et al. (1990) used a weighted average approach for their *Pinus radiata* D. Don proposed the standard number of measurement points to be 10 per tree. Cermak et al. (2004) and Jimenez et al. (2000) proposed using a number of sensors ranging from as little as 2 up to 12 depending on the tree wood anatomy and the occurrence of xylem damage or shaded suppressed trees.

The primary objectives of the present study are to: (1) quantify the spatial variability of SFD for a subtropical conifer species based on a high-resolution dataset; (2) investigate how the wood anatomy may affect the SFD; and, (3) assess and implement a suitable strategy enabling a satisfactory measurement of tree scale SFD (whole tree transpiration) with the minimum number of sensors.

Materials and methods

Site description, period of study

The study was conducted within a pine plantation [*Pinus elliottii* var. *elliottii* × *caribaea* var. *hondurensis* (PEE × PCH)] situated in Southeast Queensland, Australia (26°58′55″E, 152°58′55″E) covering 41,400 hectares. Plantation trees in our study area were 15 years old at the time of the study with mean diameter at breast height

Table 1 Review of sap flux density profiles for coniferous species observed by previous authors

References	Species	Region	Climate	Tree age	Profile
Mark and Crews (1973)	*Pinus contorta*	Colorado, USA	Alpine	Not given	Gaussian (n.g.)
Hatton et al. (1990)	*Pinus radiata*	Canberra, Australia	Dry continental	Not given	Monotonic (n.g.)
Dye et al. (1991)	*Pinus patula*	Transvaal, South Africa	Humid subtropical	4, 7 years old	No pattern (RSD = 100 %)
Čermák et al. (1992)	*Picea abies*	Sweden	Humid continental	23 years old	Gaussian (RSD = 30–45 %)
Anfodillo et al. (1993)	*Pinus sylvestris*	Dolomites, Italy	Alpine	70 years old	Bimodal (n.g.)
Koestner et al. (1996)	*Pinus sylvestris*	Upper Rhine Valley, Germany	Dry continental	35 years old	Asymmetric (n.g.)
Nadezhdina et al. (2002)	*Pinus sylvestris*	Antwerpen, Belgium	Maritime temperate	68 years old	Asymmetric (RSD = 57 %)
Ford et al. (2004b)	*Pinus* spp.	South Georgia, USA	Humid subtropical	32 years old	Asymmetric (RSD = 66 %)
Delzon et al. (2004)	*Pinus pinaster*	Landes, France	Oceanic	10, 32, 54 and 91 years old	Monotonic decrease (RSD = 80 ± 14 %)
Irvine (2004)	*Pinus ponderosa*	Cascade Mountains, USA	Alpine	25, 90 and 250 years old	Monotonic decrease (n.g.)
Fiora and Cescatti (2006)	*Abies alba*	North-Eastern Italy	Alpine	Not given	Monotonic decrease (RSD = 31–41 %)
	Picea abies	North-Eastern Italy	Alpine	Not given	Monotonic decrease (RSD = 34–47 %)
Cermak et al. (2008)	*Pinus sylvestris*	Brasschaat, Belgium	Maritime temperate	71 years old	Asymmetrical (n.g.)
Fiora and Cescatti (2008)	*Picea abies*	North-Eastern Italy	Alpine	35 years old	Monotonic decrease (RSD = 93 ± 9 %)
Cohen et al. (2008)	*Pinus halepensis*	Israel	Semi-arid and Sub-humid Mediterranean	15, 19 years old	Asymmetric (RSD = 37–73 %)
Alvarado-Barrientos et al. (2013)	*Pinus patula*	Central-Eastern Mexico	Semi-arid Mediterranean	10–34 years old	Unimodal, asymmetrical (RSD = 66–100 %)

RSD relative sapwood depth, i.e. sapwood depth over total xylem width

(DBH) of 286 ± 35 mm, a mean canopy height of 16 m and a stand density of approximately 450 trees per hectare. The surface geology, with an elevation of 33 m above sea level, is dominated by coastal quaternary deposits of sand (0–1.5 m) with an underlying weathering surface consisting of cemented sand with iron nodes (Cox et al. 2000). The sandy soil mainly consists of quartz grains with a higher organic content in the topsoil (0–0.2 m). A shallow periodically perched aquifer with varying depth occurs above the cemented sand layer. The aquifer forms during and after periods of intense rainfall (generally above 40 mm per event).

In this study, six trees were selected with a diameter at breast height (1.4 m above ground) ranging from 249 to 303 mm (Table 2). Trees were continuously monitored over periods of several days between April and June 2011 (Table 2). Trees were instrumented successively as our setup only allowed us to monitor one tree at a time. Following the measurements the trees were felled in September 2011.

Atmosphere, soil moisture and groundwater

Net radiation (Rn) was monitored using a CNR4 at 4 m above the ground (Kipp and Zonen, Delft, The Netherlands) and air temperature (*T*) and relative humidity (RH) were monitored with a Vaisala WTX510 at 2 m above the ground (Vaisala, Upsala, Finland). Vapour pressure deficit (VPD) was computed following Steppe (2004). Rn, *T* and RH were monitored 200 m from the forest in an open field at 1 min intervals and the 10 min average stored at the end of the period on a CR3000 logger (Campbell Sci., Logan, USA).

Surface soil water content was measured at 10 and 30 cm beneath the soil surface close to the instrumented trees with two time-domain frequency soil moisture probes

Table 2 Trees diameter at breast height (DBH), mean sapwood depth (averages of all cardinal directions), and monitoring periods

Tree number	DBH [mm]	Mean sapwood depth [mm] (% of the DBH/2)	Monitoring periods
1	270	126 (93 %)	14/04/11–21/04/11
2	249	106 (85 %)	22/04/11–04/05/11
3	303	134 (88 %)	05/05/11–14/05/11
4	283	114 (80 %)	19/05/11–26/05/11
5	280	123 (88 %)	01/06/11–08/06/11
6	303	126 (83 %)	09/06/11–21/06/11

(MP406, ICT International, Australia) at 1 min intervals and stored every 10 min on an ICT Smart Logger (ICT International, Australia). Groundwater level on site was monitored using a pressure transducer (Aquatroll, In situ, USA) in a hand-augered well at ~1.5 m beneath the soil surface and pressure was corrected from barometric effects.

Sap flux density probe design and configuration

The heat field deformation (HFD) method relies on heat diffusion processes within the tree stem, namely temporal temperature changes measured around the central needle of the HFD sensor, which is inserted into the tree stem and continuously heated (Nadezhdina et al. 1998). The HFD sensor includes a heating needle, with two symmetrical axial needles above and below it, as well as a tangential needle. This configuration enables the estimation of reverse and zero flow conditions. Usually, the measuring needles of the HFD sensor have several thermocouples installed 5–15 mm apart depending on the version of the sensor, which permit monitoring of the radial pattern of SFD across the xylem. The four probes used in our study were manufactured by ICT International (Armidale, Australia) and the measuring needles included either six thermocouples (at 10, 20, 30, 40, 50 and 60 mm from the base of the needles) for two of them, or eight thermocouples for the other two (at 10, 20, 30, 40, 50, 60, 70 and 80 mm from the base of the needles). The calculation of sap flux density SFD_i ($10^3 \times \mathrm{mm}^3 \times 10^{-2}\ \mathrm{mm}^{-2}\ \mathrm{h}^{-1}$) at each of the thermocouple positions i, is based on a relation between an empirical temperature ratio and the SFD (Vandegehuchte and Steppe 2013) following Nadezhdina et al. (1998) and Nadezhdina et al. (2012):

$$\mathrm{SFD}_i = 3600 \times D_{\mathrm{st}} \times (K + \mathrm{dT}_{s-a}) \times \mathrm{dT}_{as}^{-1} \times Z_{\mathrm{ax}} Z_{\mathrm{tg}}^{-1} \times L_{\mathrm{sw}}^{-1} \quad (1)$$

where D_{st} is the thermal diffusivity of the sapwo s^{-1}), K is the absolute value of $\mathrm{dT}_{\mathrm{sym}} - \mathrm{dT}_{\mathrm{asym}} \times (\mathrm{dT}_{\mathrm{s\text{-}a}})$ (°C) for the conditions when zero sap flow occurs. $\mathrm{dT}_{\mathrm{asym}}$ (respectively, $\mathrm{dT}_{\mathrm{sym}}$) is the temperature difference between the asymmetrical thermocouple positions (the symmetrical thermocouple positions). Z_{ax} is the 5 mm distance between the upper position of the axial thermocouple and the heater. Z_{tg} is the 15 mm distance between the upper position of the tangential thermocouple and the heater and L_{sw} is sapwood width (mm). Reverse sap flow was not observed during our experiment. Part of the tree bark was removed so that the first measurement point of the multi-point sensors falls at approximately 5 mm in depth from the cambium.

Because of the limitation of having only four probes, the six trees were instrumented and their SFD monitored one after another, for approximately a week each (Table 2) to increase the chance of having similar environmental conditions. SFD was sampled at 10 Hz and the average stored every 10 min. One HFD probe was installed on each of the northern, eastern, southern and western sides, respectively, at breast height above ground (1.4 m) on each tree. This setup enables simultaneous measurements of SFD at six depths for the four cardinal directions (24 measurements). The measurement points at 70 and 80 mm for the probes with 8 thermocouples were not used to upscale SFD_i to the total tree SFD to maintain consistency in the upscaling procedure with all cardinal directions. However, the maximum relative SFD at these depths is shown in Fig. 1.

After the six trees were monitored, they were felled and cross-sections at the level of the HFD sensors' locations were sampled. Locations of earlywood and latewood, as well as the sapwood–heartwood boundary were determined by visual observations (Guyot et al. 2013) using the distinct color patterns: dark (LW) or white (earlywood–latewood), and white to dark orange (sapwood–heartwood).

Selection of the dataset

All measurements were done at the beginning of the local dry season (autumn). Each period of measurement for a tree was filtered so that only 2 days of sunny conditions were selected (Table 2). Sunny conditions were based on an average daily net radiation above 175 $\mathrm{W/m^2}$ and the absence of an amplitude difference in net radiation between 10 min time steps larger than 30 $\mathrm{W/m^2}$ during these days to remove slightly cloudy days. Data were filtered to consider only daily values from 6 am to 6 pm local time. Rn is slightly higher for T1 and T2 (225 ± 190 $\mathrm{W/m^2}$/day) than for the other trees (186 ± 153 $\mathrm{W/m^2}$/day), as the measurements were done at the beginning of the

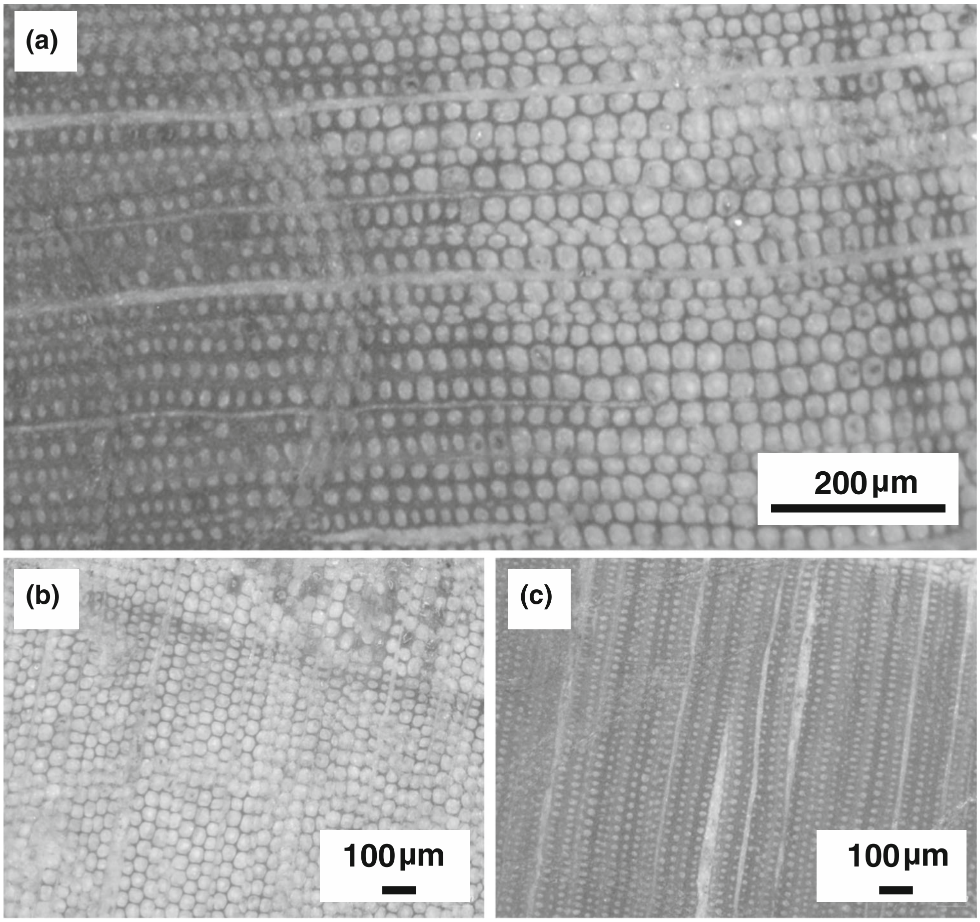

Fig. 1 Photographs of the sapwood cross-section of one of the measured trees (T5). **a** Transition between latewood (*left*) and earlywood tracheids (*right*), **b** earlywood tracheids interrupt by a thin latewood band, **c** latewood tracheids

experiment in autumn when the incoming radiation is the strongest. The average VPD for all periods is very similar; only slightly less variability was seen for T3 and T4 (1.4 ± 0.3 kPa) as compared to the other trees (1.3 ± 0.6 kPa).

Soil water content varied little during the experiment (from 16 to 20 % at 10 cm beneath the surface, and 22 to 20 % at 30 cm beneath the surface). Groundwater level was at −0.69 cm Australian Height Datum (AHD) at the start of the experiment and at −0.78 cm AHD at the end of the study.

Data processing

Following Saveyn et al. (2008), the daily maximum SFD has been normalized by the daily maximum SFD at 10 mm in depth from the cambium for each profile, to enable comparison of SFD between cardinal directions, trees, and depth in the sapwood from the cambium, and is plotted in Fig. 2.

To upscale the locally measured SFD_i (cm^3 cm^{-2} h^{-1}) to the whole tree transpiration (cm^3 h^{-1}), we followed a "weighted average approach" as per Hatton et al. (1990) and Nadezhdina et al. (2002). We converted SFD_i to sap flow per annuli by multiplying the SFD_i by the corresponding annulus area (A_i). The annulus area A_i was determined as:

$$A_i = \pi R_E^2 - \pi R_I^2 \qquad (2)$$

where R_E is the external radius and R_I the internal radius of the annulus. These radii were determined as: (i) for the outermost annulus, R_E is the cambium and R_I is the midpoint between the outermost SFD_i position and the SFD_{i+1} further in depth from the cambium; (ii) for the inner annuli, R_E as the midpoint between the SFD_i associated to that annulus and the previous external SFD_i, and R_I as the midpoint between the SFD_i associated to that annulus and the next SFD_i in depth from the cambium; (iii) for the innermost annulus, R_E as the midpoint between the SFD_i associated to that annulus and the previous external SFD_i and R_I as the sapwood–heartwood boundary. The total sap flow for the whole tree (SF_t) was then determined by adding all annuli flows following:

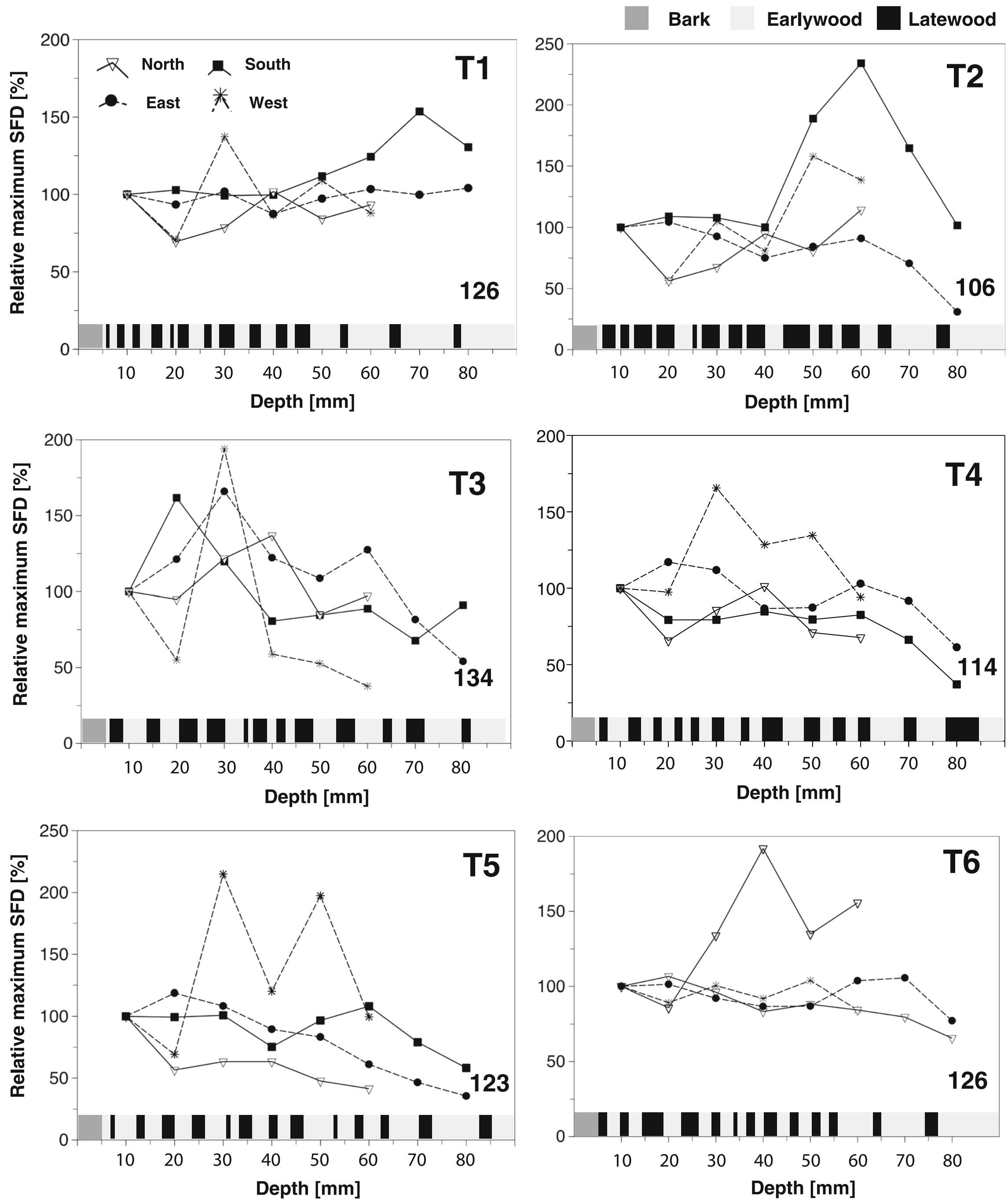

Fig. 2 Normalized profiles of sap flux density (SFD) for the six selected trees. Bark, earlywood and latewood have been measured along the needle based on cut tree stem cross-section, and are shown at scale at the bottom of the graphs. Sapwood depth is also shown on each graph

$$SF_t = \sum_{i=1}^{i=n} SFD_i A_i \quad (3)$$

The daily total sap flow (D_SF_t, $cm^3\ d^{-1}$) was then calculated by integrating the total sap flow for a given time t, (SF_t) over a two-day time-period following:

$$D\_SF_t = \int_{t=0}^{t=2\mathrm{days}} SF_t dt/2 \quad (4)$$

The daily total sap flow (D_SF_t) was calculated for 21 scenarios (Table 3). Scenarios were based on varying the number of SFD_i used for the upscaling. Two options are considered: (i) a varying number of SFD_i in depth from the cambium and (ii) a varying number of SFD_i at stem cardinal positions in which the probes were installed (North, East, South and West) (Table 3). The benchmark dataset or reference value of daily total sap flow was determined from

Table 3 Description of each scenario '*i*' and the corresponding transpiration estimate SC(*i*) based on the number and type of measurement points considered for estimating the tree transpiration

Scenario *i*	Description	Number of measurement points
1	N123456 S123456 E123456 W123456	24
2	N12345 S12345 E12345 W12345	20
3	N1234 S1234 E1234 W1234	16
4	N123 S123 E123 W123	12
5	N12 S12 E12 W12	8
6	N1 S1 E1 W1	4
7	N123456	6
8	N12345	5
9	N1234	4
10	N123	3
11	N12	2
12	N1	1
13	N123456 S123456	12
14	N12345 S12345	10
15	N1234 S1234	8
16	N123 S123	6
17	N12 S12	4
18	N1 S1	2
19	N135 S135 E135 S135	12
20	N135 S135	6
21	N135	3

Numbers after the upper case cardinal directions correspond to the depths of the sensors on each probe, e.g. N12 S12 indicates that the measurements of points at 10 and 20 mm from the probe base (at 5 and 15 mm depth), for both north and south directions have been considered for the calculation of SC(17). SC(1) is the benchmark whole tree transpiration used as the reference

N north, S south, *E* east, *W* west

calculations made from scenario 1, which consists of measurements of 24 sensors installed in the four cardinal stem locations.

To compare the total sap flow between the trees, we decided to normalize the total daily tree sap flow (D_SF_t). For this, we created an index Ix:

$$I_x = \left| \frac{(D\_SF_{Ref} - D\_SF_{SC(i)})}{D\_SF_{Ref}} \right| \quad (5)$$

where D_SF_{Ref} is the daily sap flow estimate based on the reference scenario 1 (SC(1), using the 24 sensors), and $D\_SFD_{SC(i)}$ the daily sap flow estimate based on a given scenario *i*. For each scenario, results were averaged for the six trees (with the assumption that environmental conditions are similar for the datasets) and quartiles of that average were calculated (Fig. 3).

Xylem analyses

Mean sapwood thickness was measured on the tree stem cross-sections at each sensor location (i.e. at each cardinal direction) and averaged for the four cardinal directions to generate an estimate of the cross-sectional sapwood area (Table 2). To determine the variation in tracheid size and density across the radial profile, microscopic analyses were conducted. An Olympus SZH10 microscope (Tokyo, Japan) in combination with Image Pro Plus version 5.0.1 248 (MediaCybernetics, Maryland, USA) was used to measure variation in tracheid size and density across the sapwood. Figure 1 presents different views of the tracheids' sizes, for earlywood and latewood. The eastern profile of one of the sampled trees (T5) was randomly selected for that purpose. Eight consecutive early- and latewood sample points were chosen, progressing from the cambium to the heartwood. Both the longest (a) and shortest (b) axis of 200 tracheids were measured and we calculated tracheid diameter following (Lewis 1992), where tracheid diameter $= 2 \times (ab)/(a + b)$. We also calculated tracheid density as tracheid density = number of tracheids/mm^2 (Table 4). We measured rectangles for each tracheid density calculation.

Results

Observations of SFD spatial variability

For most of the trees and cardinal directions, no particular pattern in SFD across the radial profile is observed (Table 1; Fig. 2). Some of the profiles show a strong variation of the daily maximum SFD from the cambium to the heartwood (average of 35 ± 23 percentage point difference

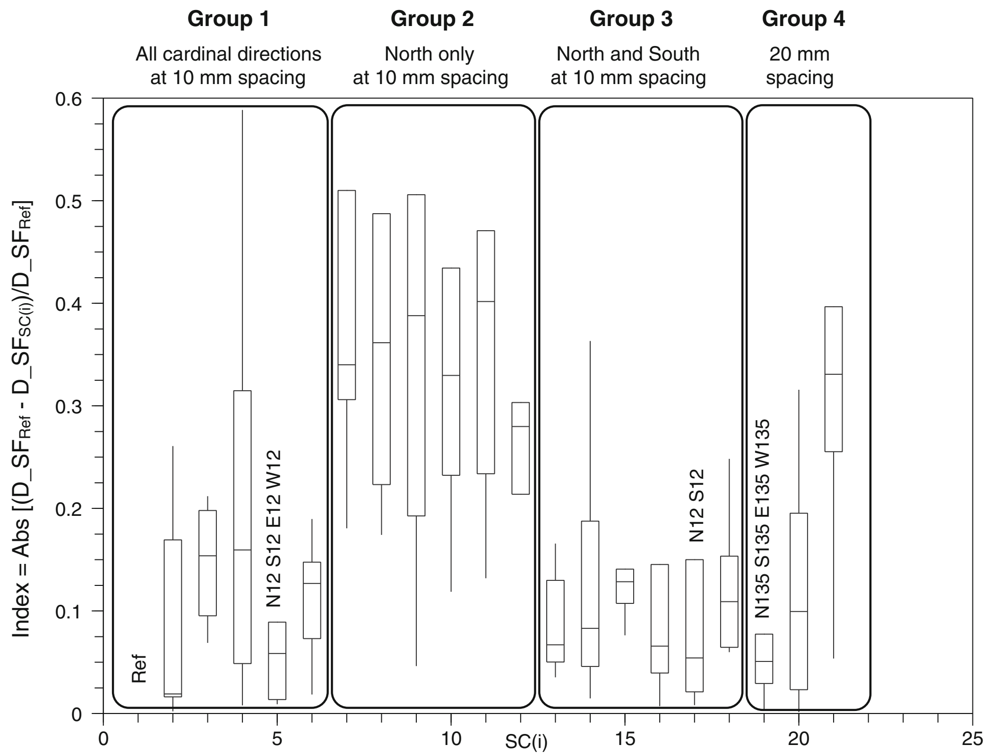

Fig. 3 Quartiles of the Index Ix for the 21 scenarios; Ix = Abs [$(D\_SF_{Ref} - D\_SF_{SC(i)})/D\_SF_{Ref}$), where D_SF_{Ref} is the daily sap flow estimate based on the reference scenario SC(1). Best sensors' configurations (SC(5), SC(17) and SC(19)) have been highlighted

Table 4 Tracheid diameters (mean ± standard error) and tracheid density for the eastern profile of tree number 5

Sapwood depth (mm) [ring type]	Conduit diameter (μm)	Conduit density (#conduits/mm^2)
10 [EW]	39.4 ± 4.0	578
10 [LW]	20.8 ± 2.8	581
20 [EW]	43.9 ± 5.3	501
20 [LW]	20.7 ± 3.0	581
30 [EW]	39.2 ± 5.5	478
30 [LW]	21.1 ± 3.2	556
40 [EW]	42.2 ± 4.4	532
40 [LW]	32.8 ± 4.3	569
50 [EW]	39.9 ± 5.1	482
50 [LW]	19.6 ± 4.2	571
60 [EW]	41.6 ± 5.5	510
60 [LW]	24.8 ± 4.9	606
70 [EW]	42.0 ± 6.0	484
70 [LW]	18.1 ± 2.4	564
80 [EW]	45.3 ± 6.3	473
80 [LW]	25.4 ± 5.1	580

EW earlywood, *LW* latewood

from one measurement point to its neighbor for all profiles, but ranging between 1 to 190 percentage point difference). Least variation occurs from 10 to 40 mm (average of 15 ± 12 percentage point difference between neighboring measurement points). A decrease of the relative maximum SFD occurs for most trees after 70 mm in depth. For all six trees, the HFD measurements indicate a persistent flow at 80 mm from the cambium (Fig. 2).

Xylem analyses

The tracheid conduit diameters were on average two times larger for earlywood (42 ± 2 microns) than for latewood (23 ± 5 microns), and the densities were lower for earlywood (505 ± 35 c/mm^2) than for latewood (576 ± 15 c/mm^2) (Table 4). For most of the trees, we observed between 10 and 12 rings of ≈5–7 mm width (composed of

≈4–5 mm of earlywood and ≈ 2–4 mm of latewood) (Fig. 2) within the outermost 70 mm of the stem radius.

Point measurement approaches based on a benchmark dataset

The performance of daily tree transpiration is evaluated against the reference dataset for the 20 monitoring scenarios, merged into four groups to facilitate the description (Fig. 2). All scenarios based on only one cardinal direction used to determine tree sap flow (group 2), exhibit the highest values of the index [Eq. (5)] with the largest quartiles, showing a great variability in tree transpiration. If an additional cardinal direction is included (group 3), the index is on average much lower, even if considering one depth only (scenario 18). The increase in the number of measurement points does not imply a decrease in the index (group 1). As an example, scenario 6 with 4 measurement points, presents a lower index with a smaller standard deviation (Ix = 0.13) than scenario 4 with 12 measurement points (Ix = 0.28). Indeed, scenario 19 with 20 mm spacing, including as well 12 measurement points gives a lower index than scenario 4. A more adequate placement of the measurement points, to capture variations in flow within the largest cross-sectional area, seems more appropriate than a high density of measurement points closer to the bark. However, this observation could be due to the very deep sapwood for our trees, and in other contexts, such as a high sap flow density close to the cambium decreasing sharply towards the heartwood, a high density of measurement points close to the cambium might be more appropriate. From all our scenarios, three provides the best scores with an average Ix below 0.05, and with a standard deviation of less than 0.05 with Ix (scenario 19) < Ix (scenario 17) < Ix (scenario 5). When scenario 19 has the best score, it is the most demanding in terms of measurement points (12). Scenario 17 (4 measurement points) is also better than scenario 5 (8 measurement points) but presents larger quartiles.

Discussion

Anatomical traits and their potential effect on sap flow measurements

Our measurements show considerable variability in SFD across the tree stem and for the different trees. Phillips et al. (1996) determined that the sapwood specific gravity could affect the SFD for coniferous species. They found that a reduction of 59 % of the daily SFD from outer to inner sapwood was accompanied by a reduction of 9 % in the specific gravity. They hypothesize that this modification of the specific gravity indicates a transition from juvenile to mature sapwood. This could explain the relatively lower flow rates observed at depths greater than 70 mm from the cambium in our study.

The variability of SFD at depths between 5 and 70 mm, with SFD varying in most cases between 20 and 50 % at rates up to 260 % for two neighboring measurements, must have another cause: our trees have very thick sapwood as compared to the trees studied by Phillips et al. (1996) and very high growth rates leaving the sapwood from 5 to 70 mm most likely juvenile. Domec and Gartner (2002) measured under laboratory conditions a specific hydraulic conductivity on average 11 times greater in earlywood as compared to the latewood tissues for a 21-year-old *Douglas Fir* (a non-porous coniferous species). Dye et al. (1991) used in situ heat pulse velocity sap flow sensors in *Pinus patula* and discovered minima and maxima of SFD correlated with latewood and earlywood, respectively. However, the widths of the early and latewood rings were of 5–10 mm and of 10–27 mm, respectively, which are large enough that the sensor could have been installed unambiguously in early and latewood. The manufacturer of the sap flow sensors used in our study (ICT International, Australia) claims an average spatial resolution of ±0.3 cm around the needle thermocouple, which means a surface resolution of 0.36 cm^2. This covers in our case several rings of earlywood and latewood. As a consequence, each of our point SFD measurements is an average of the SFD passing through earlywood and latewood tissue. Therefore, the measured average SFD will be influenced by the relative proportion of earlywood to latewood, with potentially very different specific hydraulic conductivities (Domec and Gartner 2002). These relative proportions can thus explain the local variability of SFD from one measurement point to another. Furthermore, the properties of heat diffusion and water flow in heterogeneous medium might differ from the homogeneous case for which the sap flow sensors (including HFD) have been tested and the theory established, and we might be in a case where we reached their limitations [including a constant thermal diffusivity of the sapwood in the HFD Eq. (1)].

On the strategy to install sap flow sensors

In our case of subtropical conifers, we found that the "ideal" number of sensors per tree is twelve (a loss of 2 to 7 % of accuracy as compared to the reference), a number similar to that deduced by Hatton et al. (1990), Koestner et al. (1998), Cermak et al. (2004) and Jimenez et al. (2000). It is worth noting that these authors worked with trees of different species, of different ages, and growing in different climates. Cermak et al. (2004), Nadezhdina et al. (2002) or Ford et al. (2004a, b) proposed reducing the number of sensors required by placing these at specific locations, usually close to the cambium where a peak in SFD is expected (Nadezhdina et al. 2002) and using a function to describe the SFD pattern across the xylem. However, the large variability of SFD profiles in our case prevented such an approach.

We also showed that it is possible to reduce the number of sensors to four in an "optimal" setup with two locations around the stem, without significantly compromising the accuracy of the measurement (a loss of 3–15 % accuracy as compared to the reference dataset). For long-term monitoring of transpiration, involving the deployment of sap flow sensors, there is usually a trade-off between precision and cost to achieve the best accuracy in transpiration estimate, which would depend on the number of sensors deployed to capture the spatial variability in SFD across the tree stem. On one hand, the sensors based on the Heat Field Deformation method are able to capture the spatial variability in SFD across the tree stem, but they are usually more expensive than other types of sensors, and require a larger source of energy, making them more costly and time consuming for field experiments (Nadezhdina et al. 2012; Steppe et al. 2010; Vandegehuchte and Steppe 2012). On the other hand, sensors based on the heat ratio method (HRM) (Vandegehuchte and Steppe 2012) could be manufactured at very low costs reaching only 2 % of the cost of commercial sensors (Davis et al. 2012), and could be used for long-term monitoring, placed at "optimized" locations based on a pre-monitoring phase done with HFD sensors. Therefore, a combination of these two techniques, involving pre-monitoring with HFD and long-term measurements with HRM would be the most reliable and cost-effective strategy. That is, our study supports a protocol in which a detailed survey of SFD is first established, followed by a simpler and more cost-effective deployment of HRM sensors. The latter should permit a monitoring strategy incorporating a larger, more representative selection of trees.

Given that this study presents results for subtropical conifer species with large sapwood depths, the applicability of our results to other kinds of wood architecture, specifically for ring and/or diffuse porous species, is questionable. Sapwood depth, wood properties and heterogeneities might affect the whole sap flow density spatial variability and thus lead to a different result in terms of instrumental strategy of where to install the sensors. However, a similar protocol involving an assessment of the sap flux density with a reference dataset can be easily applied to other species.

The presence of heterogeneous sapwood anatomy (in terms of conduit diameters, specific hydraulic conductivities, relative water content) raises questions on the applicability of sap flow theory. There is a need for a better quantification of the area (footprint) the sap flow sensor is actually sampling, as this area will vary depending on the sapwood anatomy. Studies on modeling of heat diffusion and conduction and water flow and storage in heterogeneous woody materials are definitely needed.

Conclusion

This study contributes to our knowledge of the optimal probe deployment strategy and monitoring practice in the field of sap flow research, in particular for conifers. Our approach of first establishing a reference benchmark dataset of tree sap flux density patterns across the sapwood, and then reducing the number of measurement point needed based on that benchmark, could be a systematic approach to unknown situations, where the sap flow variability within the trees is not known beforehand.

Author contribution statement A.G. did the analysis and the interpretation of the data. A.G. wrote the paper. A.G., K.O., J.F. and D.L. designed the study. A.G, K.O. and J.F. performed the measurements and processed the data. N.S. performed the microscopic analyses of the xylem.

Acknowledgments The authors would like to thank Alexis Gertz, Mothei Lenkopane, Amy White, Yanzi Xiao and Chenming Zhang for their help during the fieldwork, in particular for the harvesting day. The authors would also like to thank ICT International for their feedback about the instruments. We acknowledge the insightful suggestions from the associate editors and the three anonymous reviewers. The National Centre for Groundwater Research and Training is a co-funded Centre of Excellence of the Australian Research Council and the National Water Commission. Forestry Plantation Queensland supported the work by allowing access to instrument the site and graciously offering the trees.

Conflicts of interest The authors declare that they have no conflicts of interest.

References

Alvarado-Barrientos M, Hernandez-Santana V, Asbjornsen H (2013) Variability of the radial profile of sap velocity in *Pinus patula* from contrasting stands within the seasonal cloud forest zone of Veracruz, Mexico. Agric For Meteorol 168:108–119

Anfodillo T, Sigalotti G, Tomasi M, Semenzato P, Valentini R (1993) Applications of a thermal imaging technique in the study of the ascent of sap in woody species. Plant Cell Environ 16:997–1001

Brauman KA, Daily GC, Duarte TKE, Mooney HA (2007) The nature and value of ecosystem services: an overview highlighting hydrologic services. Annu Rev Environ Resour 32:67–98

Brown A, Podger G, Davidson A, Dowling T, Zhang L (2007) Predicting the impact of plantation forestry on water users at local and regional scales. An example for the Murrumbidgee River Basin. For Ecol Manag 251:82–93

Bubb KA, Croton JT (2002) Effects on catchment water balance from the management of *Pinus* plantations on the coastal lowlands of south-east Queensland, Australia. Hydrol Process 16:105–117

Cannell MG (1999) Environmental impacts of forest monocultures: water use, acidification, wildlife conservation, and carbon storage. New Forest 17(1–3):239–262

Caylor KK, Dragoni D (2009) Decoupling structural and environmental determinants of sap velocity: Part I methodological development. Agric For Meteorol 149:559–569

Čermák J, Cienciala E, Kučera J, Hällgren JE (1992) Radial velocity profiles of water flow in trunks of Norway spruce and oak and the response of spruce to severing. Tree Physiol 10(4):367–380

Cermak J, Kucera J, Nadezhdina N (2004) Sap flow measurements with some thermodynamic methods, flow integration within trees and scaling up from sample trees to entire forest stands. Trees 18:529–546

Cermak J, Nadezhdina N, Meiresonne L, Ceulemans R (2008) Scots pine root distribution derived from radial sap flow patterns in stems of large leaning trees. Plant Soil 305:61–75

Clearwater MJ, Meinzer FC, Andrade JL, Goldstein G, Holbrook NM (1999) Potential errors in measurement of nonuniform sap flow using heat dissipation probes. Tree Physiol 19(10):681–687

Cohen Y, Cohen S, Cantuarias-Aviles T, Schiller G (2008) Variations in the radial gradient of sap velocity in trunks of forest and fruit trees. Plant Soil 305:49–59

Cox ME, Preda M, Brooke B, (2000) General features of the geosetting of the pumicestone region. Passcon 2000—Pumicetone passage and deception bay catchment conference, 9–15

Davis TW, Kuo C-M, Liang X, Yu P-S (2012) Sap flow sensors: construction, quality control and comparison. Sensors. doi:10.3390/s120100954

Delzon S, Sartore M, Granier M, Loustau D (2004) Radial Profiles of sap flow with increasing tree size in maritime pine. Tree Physiol 24:1285–1296

Domec JC, Gartner BL (2002) How do water transport and water storage differs in coniferous earlywood and latewood? J Exp Bot 53:2369–2379

Downes G, Drew D (2008) Climate and growth influences on wood formation and utilisation. South For J For Sci 70(2):155–167

Dragoni D, Caylor KK, Schmid HP (2009) Decoupling structural and environmental determinants of sap velocity Part II observational application. Agric For Meteorol 149:570–581

Dye PJ, Olbrich BW, Poulter AG (1991) The influence of growth rings in *Pinus Patula* on heat pulse velocity and sap flow measurement. J Exp Bot 42:867–870

Fiora A, Cescatti A (2006) Diurnal and seasonal variability in radial distribution of sap flux density: implications for estimating stand transpiration. Tree Physiol 27:1217–1225

Fiora A, Cescatti A (2008) Vertical foliage distribution determinates the radial pattern of sap flux density in *Picea abies*. Tree Physiol 28:1317–1323

Ford C, Goranson C, Mitchell R, Rodney E, Teskey R (2004a) Diurnal and seasonal variability in the radial distribution of sap flow: predicting total stem flow in *Pinus taeda* trees. Tree Physiol 24:951–960

Ford C, McGuire M, Mitchell R, Teskey R (2004b) Assessing variation in the radial profile of sap flux density in *Pinus* species and its effect on daily water use. Tree Physiol 24:241–249

Gebauer T, Horna V, Leuschner C (2008) Variability in radial sap flux density patterns and sapwood area among seven co-occurring broad-leaved tree species. Tree Physiol 28:1821–1830

Guyot A, Ostergaard KT, Lenkopane M, Fan J, Lockington DA (2013) Using electrical resistivity tomography to differentiate sapwood from heartwood: application to conifers. Tree Physiol 33:187–194

Hatton TJ, Catchpole EA, Vertessy RA (1990) Integration of sapflow velocity to estimate plant water use. Tree Physiol 6:201–209

Irvine J, Law BE, Kurpius MR, Anthoni PM, Moore D, Schwarz PA (2004) Age-related changes in ecosystem structure and function and effects on water and carbon exchange in ponderosa pine. Tree Physiol 24(7):753–763

Jimenez MS, Nadezhdina N, Cermak J, Domingo M (2000) Radial variation in sap flow in five laurel forest tree species in Tenerife, Canary Islands. Tree Physiol 20:1149–1156

Kennedy RW (1995) Coniferous wood quality in the future: concerns and strategies. Wood Sci Technol 29(5):321–338

Koestner B, Biron P, Siegwolf R, Granier A (1996) Estimates of water vapour flux and canopy conductance of scots pine at the tree level utilising different xylem sap flow methods. Theoret Appl Climatol 53:105–113

Koestner B, Granier A, Cermak J (1998) Sap flow measurements in forest stands: methods and uncertainties. Ann Sci For 55:13–27

Lewis A (1992) Measuring the hydraulic diameter of a pore or conduit. Am J Bot 79:1158–1161

Mark W, Crews D (1973) Heat-pulse velocity and bordered pit condition in living Engelmann Spruce and Lodgepole pine trees. For Sci 19:291–296

Nadezhdina N, Cermak J, Nadezhdin V (1998) Heat field deformation method for sap flow measurements. 4th international workshop on measuring sap flow in intact plants. IUFRO, Zidlochovice, 1998

Nadezhdina N, Cermak J, Ceulemans R (2002) Radial patterns of sap flow in woody stems of dominant and understory species: scaling errors associated with positioning of sensors. Tree Physiol 22:907–918

Nadezhdina N, Vandegehuchte MW, Steppe K (2012) Sap flux density measurements based on the heat field deformation method. Trees—structure and function 0931–1890:1–10

Oishi AC, Oren R, Stoy PC (2008) Estimating components of forest evapotranspiration: a footprint approach for scaling sap flux measurements. Agric For Meteorol 148:1719–1732

Phillips N, Oren R, Zimmermann R (1996) Radial patterns of xylem sap flow in non-, diffuse-, and ring- porous tree species. Plant Cell Environ 19:983–990

Prior L, Brodribb T, Tng D, Bowman M (2012) From desert to rainforest, sapwood width is similar in the widespread conifer *Callitris columellaris*. Trees. doi:10.1007/s00468-012-0779-3

Saveyn A, Steppe K, Lemeur R (2008) Spatial variability of xylem sap flow in mature beech (*Fagus Sylvatica*) and its diurnal dynamics in relation to microclimate. Botany 86:1440–1448

Shinohara Y, Tsuruta K, Ogura A, Noto F, Komatsu H, Otsuki K, Maruyama T (2013) Azimuthal and radial variations in sap flux density and effects on stand-scale transpiration estimates in a Japanese cedar forest. Tree Physiol 33:550–558

Steppe K (2004). Diurnal dynamics of water flow through trees: design and validation of a mathematical flow and storage model. Doctoral dissertation, Ghent University

Steppe K, De Pauw DJW, Doody TM, Teskey RO (2010) A comparison of sap flux density using thermal dissipation, heat pulse velocity and heat field deformation methods. Agric For Meteorol 150:1046–1056

Vanclay KJ (2009) Managing water use from forest plantations. For Ecol Manage 257:385–389

Vandegehuchte MW, Steppe K (2012) Interpreting the heat field deformation method: erroneous use of thermal diffusivity and improved correlation between temperature ratio and sap flux density. Agric For Meteorol 162–163:91–97

Vandegehuchte MW, Steppe K (2013) Sap-flux density measurement methods: working principles and applicability. Funct Plant Biol 40(10):1088

Wilson KB, Hanson PJ, Mulholland PJ, Baldocchi DD, Wullschleger SD (2001) A comparison of methods for determining forest evapotranspiration and its components: sap-flow, soil water

budget, eddy covariance and catchment water balance. Agric For Meteorol 106(2):153–168
Wullschleger SD, Meinzer F, Vertessy RA (1998) A review of whole-plant water use studies in tree. Tree Physiol 18:499–512
Zhang L, Zhao F, Chen Y, Dixon RNM (2011) Estimating effects of plantation expansion and climate variability on streamflow for catchments in Australia. Water Resour Res 47:W12539